

RESEARCH ARTICLE

# Nucleotide transmitters ATP and ADP mediate intercellular calcium wave communication via P2Y<sub>12/13</sub> receptors among BV-2 microglia

Pengchong Jiang<sup>1</sup>, Fulin Xing<sup>1</sup>, Bu Guo<sup>1</sup>, Jianyu Yang<sup>1</sup>, Zheming Li<sup>1</sup>, Wei Wei<sup>1</sup>, Fen Hu<sup>1</sup>, Imshik Lee<sup>1</sup>, Xinzheng Zhang<sup>1,2</sup>, Leiting Pan<sup>1,3\*</sup>, Jingjun Xu<sup>1,2</sup>

**1** The Key Laboratory of Weak-Light Nonlinear Photonics, Ministry of Education, TEDA Institute of Applied Physics and School of Physics, Nankai University, Tianjin, China, **2** Collaborative Innovation Center of Extreme Optics, Shanxi University, Taiyuan, Shanxi, China, **3** The 2011 Project Collaborative Innovation Center for Biological Therapy, Nankai University, Tianjin, China

\* [plt@nankai.edu.cn](mailto:plt@nankai.edu.cn)



**OPEN ACCESS**

**Citation:** Jiang P, Xing F, Guo B, Yang J, Li Z, Wei W, et al. (2017) Nucleotide transmitters ATP and ADP mediate intercellular calcium wave communication via P2Y<sub>12/13</sub> receptors among BV-2 microglia. PLoS ONE 12(8): e0183114. <https://doi.org/10.1371/journal.pone.0183114>

**Editor:** Vincenzo Lionetti, Scuola Superiore Sant'Anna, ITALY

**Received:** May 4, 2017

**Accepted:** July 28, 2017

**Published:** August 11, 2017

**Copyright:** © 2017 Jiang et al. This is an open access article distributed under the terms of the [Creative Commons Attribution License](https://creativecommons.org/licenses/by/4.0/), which permits unrestricted use, distribution, and reproduction in any medium, provided the original author and source are credited.

**Data Availability Statement:** All relevant data are within the paper and its Supporting Information files.

**Funding:** This work was supported by the National Natural Science Foundation of China (no. 11574165), the PCSIRT (Program for Changjiang Scholars and Innovative Research Team in University) (no. IRT\_13R29), the 111 Project (no. B07013). The funders had no role in study design, data collection and analysis, decision to publish, or preparation of the manuscript.

## Abstract

Nerve injury is accompanied by a liberation of diverse nucleotides, some of which act as 'find/eat-me' signals in mediating neuron-glia interplay. Intercellular Ca<sup>2+</sup> wave (ICW) communication is the main approach by which glial cells interact and coordinate with each other to execute immune defense. However, the detailed mechanisms on how these nucleotides participate in ICW communication remain largely unclear. In the present work, we employed a mechanical stimulus to an individual BV-2 microglia to simulate localized injury. Remarkable ICW propagation was observed no matter whether calcium was in the environment or not. Apyrase (ATP/ADP-hydrolyzing enzyme), suramin (broad-spectrum P2 receptor antagonist), 2-APB (IP<sub>3</sub> receptor blocker) and thapsigargin (endoplasmic reticulum calcium pump inhibitor) potently inhibited these ICWs, respectively, indicating the dependence of nucleotide signals and P2Y receptors. Then, we detected the involvement of five naturally occurring nucleotides (ATP, ADP, UTP, UDP and UDP-glucose) by desensitizing receptors. Results showed that desensitization with ATP and ADP could block ICW propagation in a dose-dependent manner, whereas other nucleotides had little effect. Meanwhile, the expression of P2Y receptors in BV-2 microglia was identified and their contributions were analyzed, from which we suggested P2Y<sub>12/13</sub> receptors activation mostly contributed to ICWs. Besides, we estimated that extracellular ATP and ADP concentration sensed by BV-2 microglia was about 0.3 μM during ICWs by analyzing calcium dynamic characteristics. Taken together, these results demonstrated that the nucleotides ATP and ADP were predominant signal transmitters in mechanical stimulation-induced ICW communication through acting on P2Y<sub>12/13</sub> receptors in BV-2 microglia.

**Competing interests:** The authors have declared that no competing interests exist.

## Introduction

The intracellular roles of nucleotides (ATP, ADP, UTP, etc.) have long been recognized as energy currency or building blocks for DNA and RNA. However, in the extracellular compartment, mounting evidences reveal that they function as key signal molecules to participate in various processes including inflammation, infection and tissue damage through activation of membrane P2 nucleotide receptors [1, 2]. For instance, during nerve injury, amount of ATP, ADP and UTP liberated from apoptotic neurons and acted as 'find-me' signal via activating P2Y receptors, resulting in oriented migration of microglia [3, 4]. The 'eat-me' signal such as UDP will promote phagocytic clearance of dead cells and tissue debris by microglia through activating P2Y<sub>6</sub> receptor [5, 6]. Moreover, extracellular nucleotide signaling by P1 and P2 receptors was found to regulate numerous inflammatory responses, which contributed to maintain the pro/anti-inflammatory balance of the central nervous system (CNS) [1, 7].

In the CNS, microglia acted as the first and main immune defense against infectious and pathological events [8]. They could promptly survey changes of the surroundings and sense extracellular messengers via cell surface receptors [9], subsequently congregate together rapidly to build a protective barrier between normal and damaged tissues [10]. Intercellular Ca<sup>2+</sup> wave (ICW) communication was the principal approach by which microglia [11, 12], astrocytes [13], and neurons [14] coordinate and synchronize with each other to execute immune defense and maintain homeostasis of CNS. ICWs could prefigure and guide the migration of microglia in response to neuronal damage [15].

Many reports showed that extracellular nucleotide ATP played as an important signal transmitter in ICWs [16–18]. However, it remains unclear whether and how other types of extracellular nucleotides contribute to ICW communication in microglia. In the present study, we evoked ICWs in an immortalized murine microglial cell line (BV-2) by localized micro-stimulation on single cell using glass microelectrodes. We investigated the involvement of potential intercellular messengers and corresponding receptors. Results provided compelling evidences that both ATP and ADP played pivotal roles in ICW communication via P2Y<sub>12/13</sub> receptors in BV-2 microglia, rather than other types of nucleotides.

## Materials and methods

### Cell culture

BV-2 cell is an immortalized mouse microglial cell line that exhibits the morphological and functional characteristics of microglia [19]. The BV-2 cells, a generous gift from Dr. Linhua Jiang (Institute of Membrane and System Biology, Faculty of Biological Sciences, University of Leeds, Leeds, U.K.), were routinely cultured in Dulbecco's modified Eagle's medium (DMEM, Gibco, USA) supplemented with 10% (v/v) fetal bovine serum (FBS, Biological Industries, USA), 100 U/mL penicillin and 100 µg/mL streptomycin (Gibco, USA) at 37°C under 5% CO<sub>2</sub>. Before test, cells were isolated with 0.25% trypsin + 0.04% EDTA (Gibco, USA) and plated on glass coverslips at a density of 2×10<sup>4</sup> cells/cm<sup>2</sup> to be adherent for 18 h.

### Single-cell level mechanical stimulation

Local mechanical stimulus was performed using glass microelectrodes (1 µm tip diameter), drawn by flaming/brown micropipette puller (Model P-97-6368, Sutter Instrument Co., USA). The glass microelectrodes were mounted on a Three-axis Hanging Joystick Oil Hydraulic Micromanipulator (MMO-202ND, Narishige, Japan), which was fixed on the Axio observer D1 inverted fluorescent microscope (Carl Zeiss, Germany). During fluorescence image

acquisition, the tip of the microelectrode was controlled to provoke an acute, short-lasting mechanical stimulation on target cells.

## Ca<sup>2+</sup> imaging

Measurements of cytosolic calcium concentration ( $[Ca^{2+}]_c$ ) in microglia was performed as described previously [11]. Briefly, BV-2 microglial cells were incubated with 3  $\mu$ M calcium-sensitive Fluo-4 AM (Invitrogen, USA) for 40 min at 37°C in Hanks balanced salt solution (HBSS, 140 mM NaCl, 5 mM KCl, 2 mM CaCl<sub>2</sub>, 1 mM MgCl<sub>2</sub>·6H<sub>2</sub>O, 10 mM glucose, 10 mM HEPES, pH 7.4) in the presence of 10% pluronic F-127 (Biotium, USA), subsequently washed for 10 min with HBSS for de-esterification. Ca<sup>2+</sup> dynamics was observed by the Axio observer D1 inverted fluorescent microscope. Fluo-4 was excited by a mercury with a 485/20 nm excitation filter, and fluorescence was collected by a fluar 40×/1.30 oil objective with 540/50 nm emission filter. Images were acquired by an electron multiplying charge coupled device (EMCCD) (DU-897D-CS0-BV, Andor, U.K.), which was controlled by MetaMorph software (Universal Imaging Corp., USA). Each fluorescence image was acquired for 50 ms with a 1 s interval between frames. The obtained data were quantitatively analyzed for changes of fluorescence intensities within the region of interest (ROI). The  $[Ca^{2+}]_c$  level over time was presented as relative fluorescence intensity ( $F/F_0$ , intensity after stimulation/basal intensity before stimulation).

## RT-PCR

Total RNA from BV-2 microglial cells was isolated using RNAPrep pure Cell/Bacteria Kit (Tiangen, Beijing). Then, the RNA (1  $\mu$ g) was subjected to reverse transcription (RT) using a RT system (Promega, USA) in a total volume of 20  $\mu$ l that contained MgCl<sub>2</sub> (25 mM, 4  $\mu$ l), reverse transcription 10× buffer (2  $\mu$ l), dNTP mixture (10 mM, 2  $\mu$ l), RNase inhibitor (0.6  $\mu$ l), AMV reverse transcriptase (1  $\mu$ l) and Oligo(dT) primer (1  $\mu$ l). The reaction mixtures were incubated at 45°C for 30 min, 99°C for 5 min to inactivate the enzyme, and then chilled on ice for 5 min. Subsequently, the product of RT reaction (1  $\mu$ l) was amplified using a GoTaq Green Master Mix (Promega, USA) in a total volume of 50  $\mu$ l PCR buffer containing Green Master Mix, 2× (25  $\mu$ l), sense primer (0.5  $\mu$ l) and antisense primer (0.5  $\mu$ l). The reaction mixtures were preheated to 95°C for 2 min followed by 40 thermal cycles in a PCR machine (MJMiniTM, BIO-RAD, USA). For each cycle, denaturation was at 95°C for 30 s, annealing at 63.5°C for 30 s, and extension at 72°C for 1 min. Sequences of gene-specific primers (S1 Table) were designed using the Primer 5 (Premier Biosoft, USA) and evaluated with Oligo 7 (Molecular Biology Insights, USA).

## Western blot

BV-2 microglia were seeded in a 6-well plate and lysed in 100  $\mu$ l RIPA solution (Beyotime, China). The total protein concentration was determined by BCA assay. Total protein lysates (~80  $\mu$ l) were denatured at 95°C for 10 min. Proteins (20  $\mu$ g/lane) were subjected to 8% SDS-PAGE by 80 V at room temperature for 2 h. The resolved proteins were transferred onto nitrocellulose membranes by 80 V for 1.5 h. Upon blocking non-specific binding sites with 3% BSA for 1 h at 4°C, membranes were incubated using the following primary antibodies overnight at 4°C: rabbit anti-P2Y<sub>12</sub> (1:500; 75 kDa; Alomone, Isreal) and mouse anti- $\beta$ -actin (1:1000; 42 kDa; Beyotime, China). After washing, membranes were incubated with horseradish peroxidase-labeled goat anti-rabbit (for P2Y<sub>12</sub>; 1:1000; Alomone, Isreal) and goat anti-mouse (for  $\beta$ -actin; 1:1000; Beyotime, China) secondary antibodies for 1h. Finally, bands were

visualized with the enhanced chemiluminescence (ECL; Tanon, China) and the Tanon 5200 MultiImage System (Tanon, China).

## Immunofluorescence

BV-2 microglial cells were prepared as described above and seeded on a glass cover slip in a 6-well plate (Corning, USA) for 24 h. For living cell immunostaining, cells were incubated with anti-P2Y<sub>12</sub> (extracellular) rabbit antibody (1:500; Alomone, Israel) resolved in DMEM at 37°C for 1h, followed by washing with HBSS for three times. Then, cells were stained with Alexa-488 goat anti-rabbit IgG (1:500; Abcam, UK) at 37°C for 1h. After washing with HBSS for three times, images were obtained by 535 nm emission filter based on an Olympus IX51 inverted fluorescence microscope with 40× oil objective.

## Statistical analysis

A cell was defined as responsive to mechanical stimulation if it showed a calcium transient with a peak magnitude not less than 1.1 times of baseline. The response rate was defined as the number of responsive neighboring cells (except the stimulated cell) divided by the total number of neighboring cells in each group. All data were analyzed using the IBM software SPSS (version 22). For multiple comparisons, the data were analyzed using unpaired Student's t-test and analysis of variance (ANOVA) followed by the Scheffé *post hoc* test.  $P < 0.05$  was considered statistically significant.

## Results

### Mechanical stimulation on a single BV-2 microglia initiates intercellular Ca<sup>2+</sup> wave propagations

To simulate local injury in the CNS, we mechanically stimulated BV-2 microglia using glass microelectrodes (Fig 1A). Before stimulation treatment, all cells should be in resting states indicated by stable basal [Ca<sup>2+</sup>]<sub>c</sub> ( $F/F_0 = 1$  for Fig 1B). In addition, we paid attention to keeping the integrity of plasma membrane after treatment with mechanical stress tested by propidium iodide staining (S1 Fig). Fig 1B displayed the Ca<sup>2+</sup> traces of the stimulated cell and five representative neighboring cells. Fig 1C and S1 Movie showed a typical process of ICW propagations among BV-2 microglia in response to mechanical stimulus. It can be found that mechanical stimulation triggered a rapid rise of [Ca<sup>2+</sup>]<sub>c</sub> that originated from the point of the stimulation and then spread throughout the whole cell body (Fig 1C, 1s and 2s). Upon reaching the cell boundaries, the Ca<sup>2+</sup> transient propagated to the neighboring cells in a wave-like manner, namely, intercellular calcium waves (ICWs). The velocity of these ICWs was  $10.43 \pm 2.66 \mu\text{m/s}$ .

### ICWs are mainly due to Ca<sup>2+</sup> release from intracellular stores

To verify the contribution of external Ca<sup>2+</sup>, we calculated response rate and [Ca<sup>2+</sup>]<sub>c</sub> peak value by dividing neighboring cells into four groups with different distances, that was, 0–25 μm group, 25–50 μm group, 50–75 μm group and 75–100 μm group. For Ca<sup>2+</sup>-containing condition, the response rate of ICW was  $81.7 \pm 13.7\%$  (0–25 μm group),  $72.4 \pm 20.8\%$  (25–50 μm),  $41.5 \pm 27.9\%$  (50–75 μm) and  $33.0 \pm 17.4\%$  (75–100 μm) (blue color, Fig 2A). For Ca<sup>2+</sup>-free buffer, it was  $94.3 \pm 9.0\%$  (0–25 μm),  $72.4 \pm 13.3\%$  (25–50 μm),  $51.7 \pm 19.1\%$  (50–75 μm) and  $28.3 \pm 12.3\%$  (75–100 μm) (green color, Fig 2A). There was no statistically significant difference in the response rate between the Ca<sup>2+</sup>-containing and the Ca<sup>2+</sup>-free groups. For peak value, the mean of 0–25 μm group was taken as 1, and other groups were normalized to

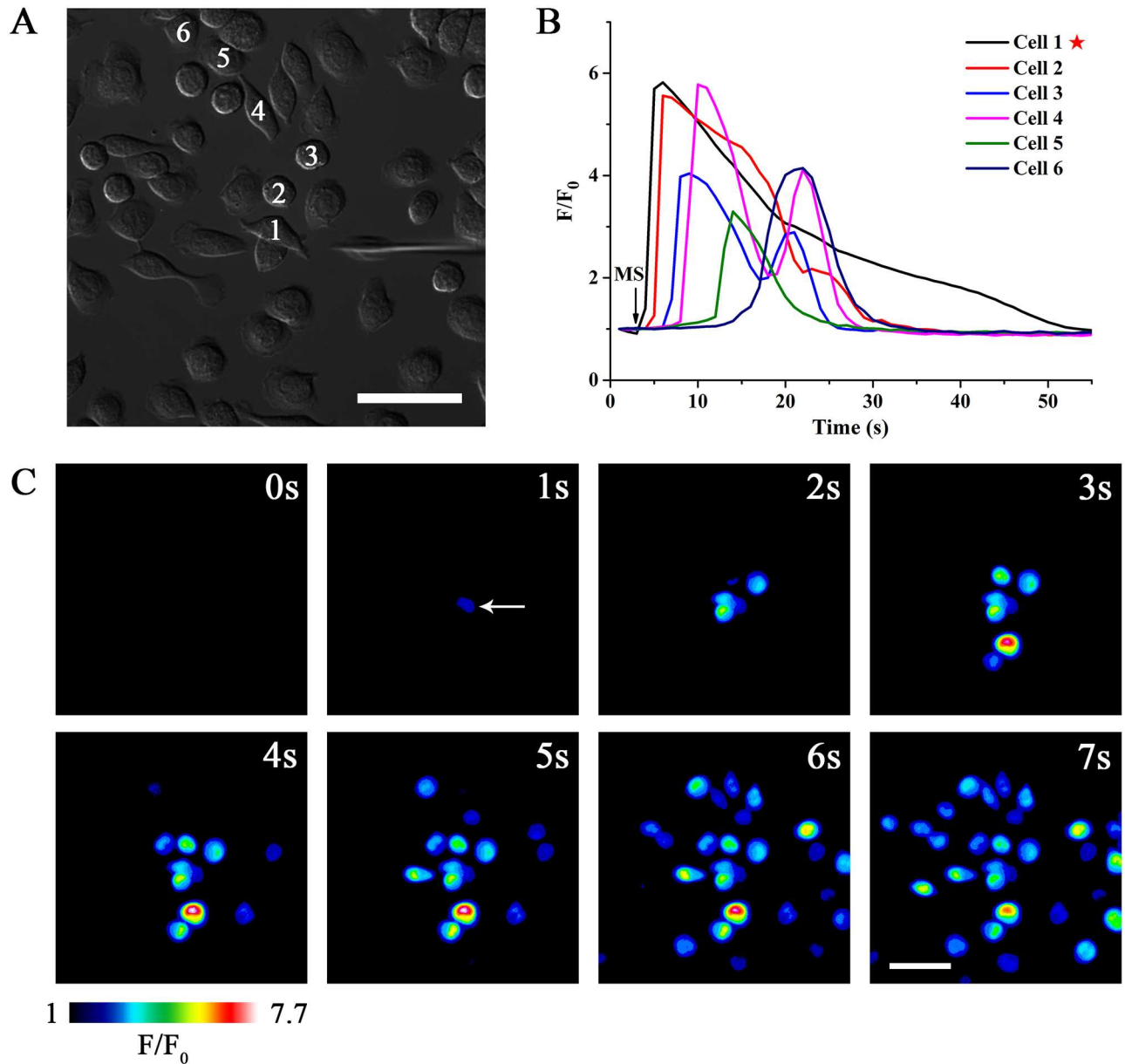


**Fig 1. Mechanical stimulation on an individual cell induces intercellular calcium wave (ICW) propagations among separated BV-2 microglia.** MS indicates the mechanical stimulation event. Pentagram indicates the stimulated cell. **(A)** Representative image of BV-2 microglia and glass microelectrode visualized by differential interference contrast (DIC) microscope. **(B)** The Ca<sup>2+</sup> traces of the stimulated cell (Cell 1) and five neighboring cells (Cell 2–6). **(C)** A sequence of pseudocolor images that show mechanical stimulation elicited-propagation of ICWs among isolated BV-2 microglia. The white arrow indicates the application of mechanical stimulation on the selected microglia. Relative changes in [Ca<sup>2+</sup>]<sub>c</sub> are depicted on a pseudocolor scale with white representing the highest and black the lowest values. Scale Bar = 50 μm.

<https://doi.org/10.1371/journal.pone.0183114.g001>

0–25 μm group. It was  $1 \pm 0.16$  (0–25 μm),  $0.86 \pm 0.19$  (25–50 μm),  $0.78 \pm 0.26$  (50–75 μm) and  $0.70 \pm 0.24$  (75–100 μm) in Ca<sup>2+</sup>-containing buffer (Fig 2B). Similarly, the peak value was  $1 \pm 0.23$  (0–25 μm),  $0.78 \pm 0.28$  (25–50 μm),  $0.68 \pm 0.28$  (50–75 μm), and  $0.66 \pm 0.21$  (75–100 μm) in Ca<sup>2+</sup>-free medium (Fig 2C). Together, we believed that ICWs resulted from mechanical stimulation did not rely on external Ca<sup>2+</sup>. To further address the calcium source of ICWs, cells were treated with 2-aminoethyl diphenylborate (2-APB, potent IP<sub>3</sub> receptor



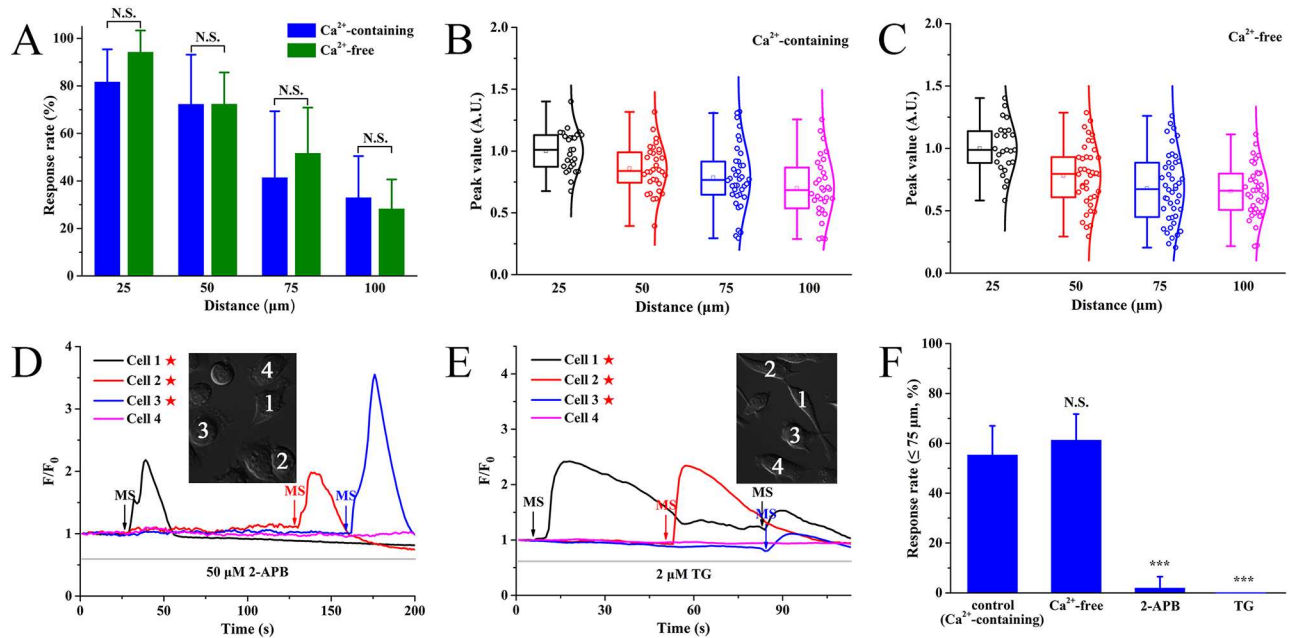


**Fig 2. Mechanical stimulation-induced ICWs were dependent on release of IP<sub>3</sub>-sensitive calcium store.** MS indicates the mechanical stimulation event. Pentagram indicates the stimulated cell. **(A)** The response rate of ICWs in the presence and absence of extracellular Ca<sup>2+</sup> (n ≥ 20 cells for each distance from five independent experiments). All values are expressed as mean ± SD. Data are statistically analyzed by the unpaired Student's t-test. N.S., no significant difference. **(B and C)** The distribution of ICW peak values (n ≥ 25 cells for each distance from six independent experiments) is shown in box plot with and without extracellular Ca<sup>2+</sup>. The mean peak value of 0–25 μm group are taken as 1, and other groups are normalized to 0–25 μm group. **(D)** Inhibition of ICWs by pretreatment with 2-APB (50 μM for 15 min). **(E)** Pretreatment with 2 μM TG for 5 min inhibits ICW propagation. **(F)** Statistical data of the response rate within 75 μm for all experimental groups (n ≥ 90 cells for each condition from at least three independent experiments). Data are statistically analyzed by one-way ANOVA followed by Scheffé post hoc test. \*\*\*P < 0.001.

<https://doi.org/10.1371/journal.pone.0183114.g002>

blocker) and thapsigargin (TG, specific inhibitor of sarcoplasmic/endoplasmic reticulum Ca<sup>2+</sup>-ATPase) prior to mechanical stimulus, respectively. Data showed that mechanical stimulus did not induce ICW propagation in the presence of 2-APB (50 μM for 15 min) (Fig 2D) or TG (2 μM for 5 min) (Fig 2E). The statistical response rate of ICWs by 75 μm was 55.4 ± 11.6% (Ca<sup>2+</sup>-containing), 61.3 ± 10.4% (Ca<sup>2+</sup>-free), 2.0 ± 4.5% (2-APB), and 0 ± 0% (TG), respectively (Fig 2F). In brief, these results indicated that Ca<sup>2+</sup> waves propagation evoked by mechanical stimulus depended on IP<sub>3</sub>-sensitive calcium store release in BV-2 microglia.

### ICW propagation is mediated by ATP-dependent P2Y purinergic signaling

Our data showed that the 1<sup>st</sup> treatment with ATP/ADP could not only strongly suppress Ca<sup>2+</sup> mobilization strength in response to the 2<sup>nd</sup> challenge, but also significantly delay response time (S2 Fig), indicating that purinoceptors could be desensitized in BV-2 cells with applications of nucleotides. Thus, to investigate whether ICWs were linked to ATP release, we applied different doses of exogenous ATP (0.3, 1 and 10 μM) prior to mechanical stimuli to desensitize corresponding purinoceptors. Results showed that ICWs were largely blocked by 0.3 μM ATP (Fig 3A), and completely suppressed by 1 and 10 μM ATP (Fig 3B and 3C). Besides, preincubation with apyrase (10 U/mL for 30 min), an ATP-hydrolyzing enzyme, evidently blocked the ICWs (Fig 3D), further demonstrating the importance of ATP during ICWs.

Because of the relevance between ATP and P2 purinergic receptors, we determined the involvement of P2 receptors by pretreatment of suramin (a broad-spectrum P2 receptor

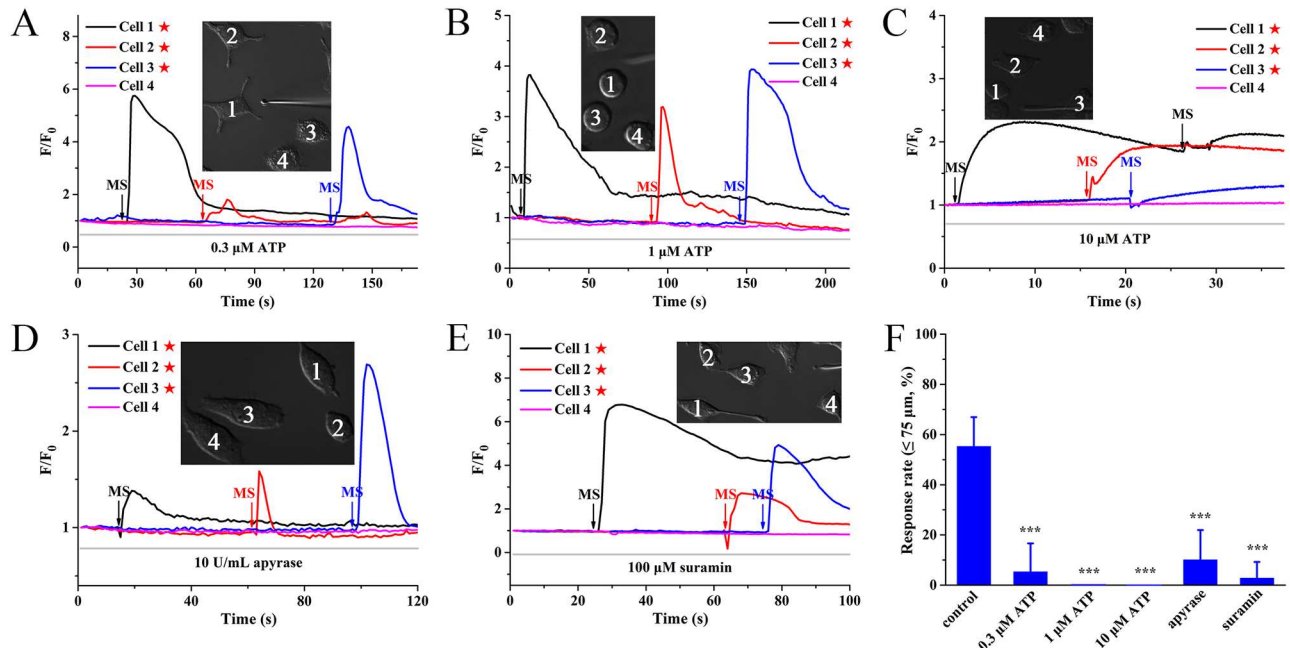


**Fig 3. Extracellular nucleotide ATP is associated with ICW propagation via P2Y receptors activation.** MS indicates the mechanical stimulation event. Pentagram indicates the stimulated cell. (A-C) Application of exogenous ATP (A: 0.3 μM; B: 1 μM; C: 10 μM) blocks mechanical stimulation-induced ICWs in a dose-dependent manner. (D) Preincubation with 10 U/mL apyrase for 15 min suppresses calcium waves. (E) Pretreatment with 100 μM suramin for 15 min abolishes ICW propagation. (F) Statistical data of the response rate within 75 μm for all experimental groups (n ≥ 90 cells for each condition from at least three independent experiments). All values are expressed as mean ± SD. Data are statistically analyzed by one-way ANOVA followed by Scheffé post hoc test. \*\*\*P < 0.001.

<https://doi.org/10.1371/journal.pone.0183114.g003>

antagonist). Results showed that ICWs were almost abolished by 100 μM suramin (Fig 3E). As summarized in Fig 3F, the response rate of ICWs (0-75 μm) was 55.4 ± 11.6% for control, 5.4 ± 11.2% for 0.3 μM ATP group, 0 ± 0% for 1 and 10 μM ATP, 10.2 ± 11.8% for apyrase and 2.9 ± 6.4% for suramin, respectively. It was known that P2 receptors could be classified into two families: ionotropic P2X ion channels, which mediate calcium influx, and metabotropic G protein-coupled P2Y receptors that initiate intracellular calcium release via IP<sub>3</sub>-sensitive calcium store [20]. Thus, considering that the ICWs were due to intracellular calcium release (Fig 2), the calcium response was mostly associated with P2Y receptors. These results together demonstrated that the mechanical stimulation-induced ICWs were mediated by extracellular nucleotides ATP via activation of P2Y subtypes in BV-2 microglia.

### The key roles of ADP and P2Y<sub>12/13</sub> receptors in microglial ICWs

We further tested the effects of other four naturally occurring nucleotides (ADP, UTP, UDP and UDP-glucose) on mechanical stimulation-evoked ICWs. Data showed that ADP could abolish ICW propagation in a dose-dependent manner (Fig 4A and 4G). In contrast, UTP (Fig 4B), UDP (Fig 4C) and UDP-glucose (Fig 4D) had no effect on these ICWs. These results suggested that ADP was also a significant signal molecule during mechanical stimulation-induced ICWs. To investigate the roles of various purinoceptors in ICW propagations, we subsequently examined the expression of different subtypes of P2Y receptors in BV-2 microglia using RT-PCR. Data showed high transcripts of P2Y<sub>12</sub> receptors, as well as significant expression P2Y<sub>2,6,13,14</sub> receptors (Fig 4H). The detailed expression rate of mRNA was 40.3 ± 11.3% for P2Y<sub>2</sub>, 40.6 ± 20.2% for P2Y<sub>6</sub>, 90.7 ± 4.0% for P2Y<sub>12</sub>, 51.4 ± 2.1% for P2Y<sub>13</sub>, and 53.6 ± 2.9% for P2Y<sub>14</sub> (Fig 4I; as the positive control, the expression of GAPDH was taken as 100%). Excluding

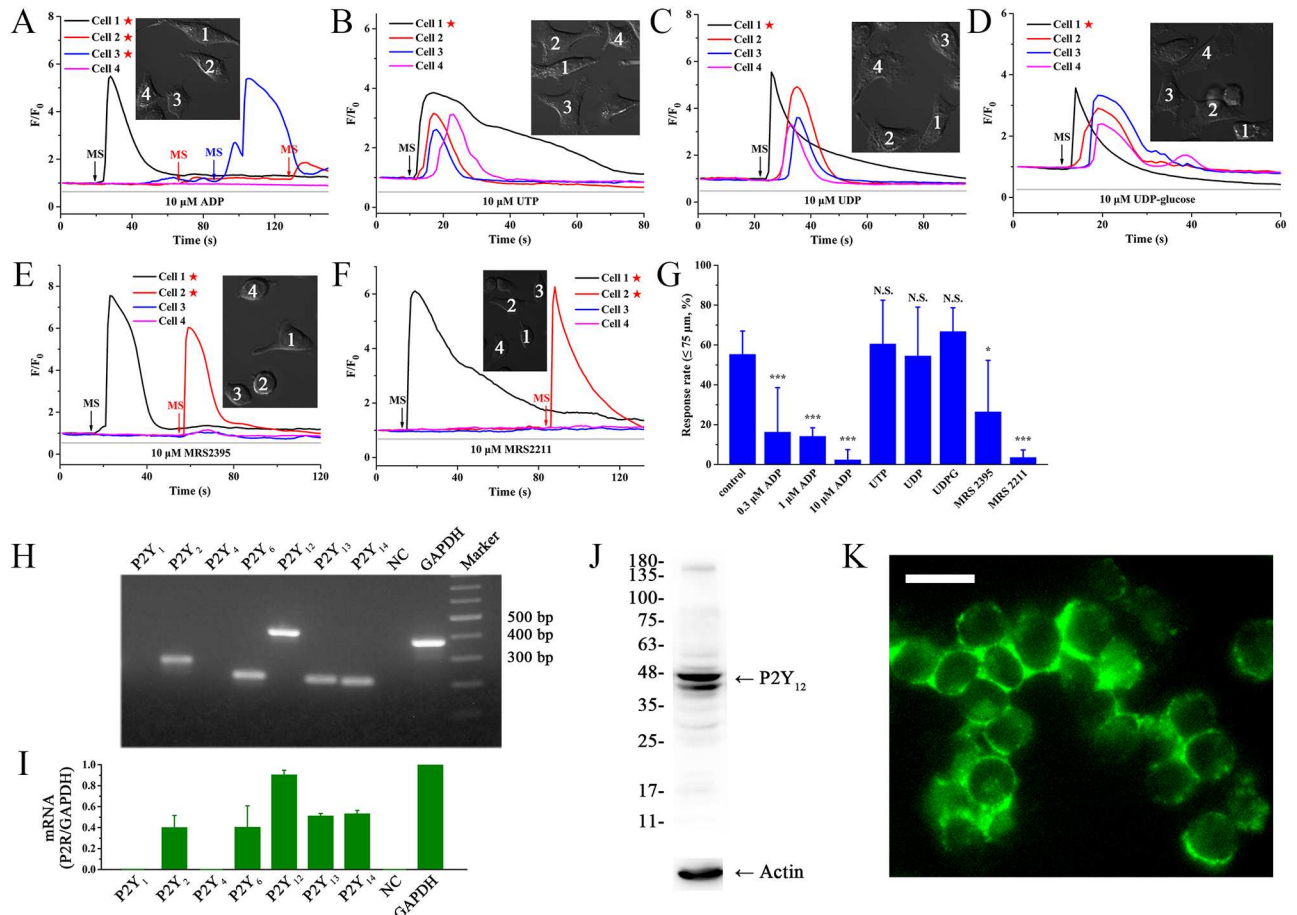


**Fig 4. ADP acts as another transmitter associated with activation of P2Y<sub>12/13</sub> receptors during ICWs.** MS indicates the mechanical stimulation event. Pentagram indicates the stimulated cell. **(A)** Application of ADP prior to mechanical stimulation blocks ICWs. **(B–D)** Application of 10 μM UTP **(B)**, 10 μM UDP **(C)** and 10 μM UDP-glucose **(D)** have no inhibitory effects on ICW communication. **(E)** Pretreatment with 10 μM for 15 min MRS2395 partially inhibits ICWs. **(F)** Preincubation with 10 μM MRS2211 for 15 min suppresses ICW propagation. **(G)** Summary inhibitory effects of nucleotides on ICWs within 75 μm (n ≥ 88 cells for each condition from at least three independent experiments). All values are expressed as mean ± SD. \*P < 0.05 and \*\*\*P < 0.001, one-way ANOVA, Scheffé post hoc test. N. S., no significant difference. **(H)** Gene expression of P2Y receptors in BV-2 microglia at mRNA level detected by RT-PCR. The ten lanes in the gel are as follows: P2Y<sub>1,2,4,6,12,13,14</sub> (experimental group with primers directed towards the P2YR mRNA); nuclease-free water (negative control); GAPDH (positive control) and marker (with a list of standardized DNA sequences from 100 bp to 800 bp). **(I)** Quantitative statistical results of RT-PCR normalized to GAPDH (n = 3). All values are expressed as mean ± SD. **(J)** Western-blot assay indicates expression of P2Y<sub>12</sub> receptor in BV-2 microglia. **(K)** Immunolocalization of P2Y<sub>12</sub> receptor on the membrane of BV-2 cells. Scale bar = 30 μm.

<https://doi.org/10.1371/journal.pone.0183114.g004>

P2Y<sub>2,4</sub> (activated by UTP), P2Y<sub>6</sub> (UDP) and P2Y<sub>14</sub> receptors (UDP-glucose), therefore, the P2Y<sub>12/13</sub> receptors, which can be activated and desensitized by ATP/ADP [21, 22], should contribute to ICWs. In order to verify the key roles of P2Y<sub>12/13</sub> receptors, we performed inhibition experiments utilizing their specific antagonists, MRS2395 (for P2Y<sub>12</sub>R) and MRS2211 (for P2Y<sub>13</sub>R). Results showed that application of 10 μM MRS2395 (15 min) could partially suppress the ICWs (Fig 4E). Meanwhile, 10 μM MRS2211 (15 min) significantly blocked these processes (Fig 4F). As summarized in Fig 4G, the response rate of ICWs (0–75 μm) was 55.4 ± 11.6% for control, 16.4 ± 22.2% for 0.3 μM ADP, 14.2 ± 4.2% for 1 μM ADP, 2.5 ± 5.0% for 10 μM ADP, 60.6 ± 21.9% for 10 μM UTP, 54.6 ± 24.4% for 10 μM UDP, 66.8 ± 11.8% for 10 μM UDP-glucose, 26.5 ± 25.8% for 10 μM MRS2395 and 3.6 ± 3.7% for 10 μM MRS2211, respectively. In



addition, we typically confirmed the presence of P2Y<sub>12</sub> receptor in BV-2 microglia using western-blot assay (Fig 4J) and immunofluorescence (Fig 4K).

### Quantitative estimation of extracellular ATP/ADP concentrations sensed by neighboring BV-2 microglia during Ca<sup>2+</sup> wave propagation

As a critical mechanism of [Ca<sup>2+</sup>]<sub>c</sub> regulation, store operated calcium entry (SOCE) can be triggered by a depletion of intracellular calcium stores. Mechanical stimulus-induced ICWs were found to depend on IP<sub>3</sub> receptor-sensitive stores release in BV-2 microglia (Fig 2). However, readdition of 2 mM external calcium did not lead to a second rising of [Ca<sup>2+</sup>]<sub>c</sub> in non-mechanically stimulated BV-2 microglia (cell 2–4 in Fig 5A), indicating the independence of SOCE. Thus, we used different concentration of exogenous ATP and ADP to mimic the pattern of calcium mobilization during ICWs. Data showed that application of 0.1 μM ATP induced a sustained and regular calcium oscillation in Ca<sup>2+</sup>-free HBSS (Fig 5B). 0.1 μM ADP only resulted in weak Ca<sup>2+</sup> responses (data not shown). Interestingly, similar to that of mechanical stimulation, application of 0.3 μM ATP (Fig 5C) and 0.3 μM ADP (Fig 5E) induced Ca<sup>2+</sup> mobilization without SOCE. In contrast, 1 μM ATP (Fig 5D) and 1 μM ADP (Fig 5F) could evoke evident SOCE. Taken together, we suggested that the concentration of ATP and ADP sensed by neighboring BV-2 microglia was about 0.3 μM during mechanical stimulation-induced ICWs.

### Discussion

ICWs appear to be a widespread phenomenon by which various cell types communicate with each other to coordinate and synchronize their activities. For instance, ICWs prefigure and guide the migration of microglia in response to neuronal damage [15], as well as regulate the functions of glial cells in inflammation and immunity [23]. In the present study, we employed mechanical stimulation to an individual BV-2 microglia, and observed remarkable ICWs among adjacent cells. Subsequently, we determined the involvement of several naturally occurring nucleotides in these ICWs. Data showed that ATP and ADP, rather than UTP, UDP and UDP-glucose, were the predominant signal messengers for ICW communication. Furthermore, we indicated that calcium waves were mostly mediated by P2Y<sub>12/13</sub> receptors.

As significant paracrine messengers in the CNS, nucleotides were known to be released in response to biochemical or physical stimuli, such as oxygen radicals, mechanical forces and virus infection [24, 25]. Nucleotides could be released from the stimulated cells through exocytosis pathway or conductive mechanisms (including pannexin channels, P2X<sub>7</sub> receptors etc.) [26–28]. The released nucleotides gradually diffused to adjacent cells, which subsequently evoked ICW propagation by activating membrane-bound P2 receptors [29]. In this study, we found that mechanical stimulation triggered remarkable ICWs among BV-2 microglia (Fig 1). Subsequently, we investigated the effects of five naturally occurring nucleotides (ATP, ADP, UTP, UDP and UDP-glucose) on the ICWs. It has been well established that prior challenge with agonists could result in desensitization of P2 receptors, especially the G protein-coupled P2Y receptors to a second challenge with the same agonists [30, 31]. Our results showed that desensitization with ATP (Fig 3A to 3C) and ADP (Fig 4A) significantly blocked mechanical stimulation-induced Ca<sup>2+</sup> waves. In contrast, application of UTP (Fig 4B), UDP (Fig 4C) and UDP-glucose (Fig 4E) did not abolish ICW propagation. Therefore, these results indicated that ATP and ADP were predominant transmitters during mechanical stimulation-induced ICW communication in BV-2 microglia.

Furthermore, according to our results, the ICWs were independent on extracellular Ca<sup>2+</sup> (Fig 2A to 2C) and relied on IP<sub>3</sub>-sensitive calcium store release (Fig 2D and 2E). Thus, it

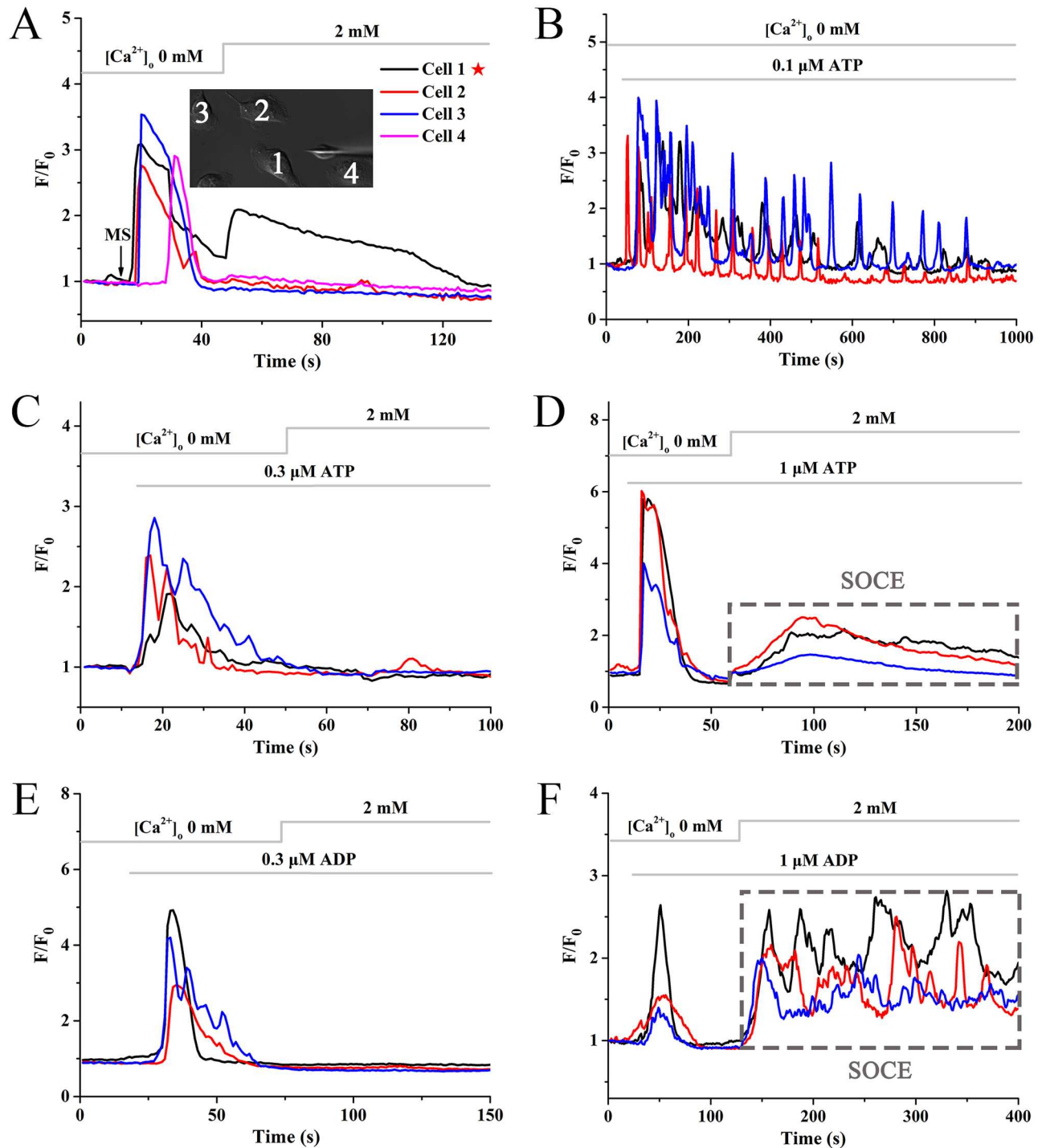


**Fig 5. Concentrations of ATP and ADP sensed by P2 receptors during ICWs.** MS indicates the mechanical stimulation event. Pentagram indicates the stimulated cell. **(A)** Mechanical stimulus is used to evoke ICWs in the absence of extracellular Ca<sup>2+</sup>, followed by re-addition of 2 mM external Ca<sup>2+</sup>. **(B)** Application of 0.1 μM ATP without extracellular Ca<sup>2+</sup>. **(C and D)** Application of ATP (0.3 and 1 μM) in the absence of extracellular Ca<sup>2+</sup> followed by replenishment of 2 mM external Ca<sup>2+</sup>. **(E and F)** Addition of ADP (0.3 and 1 μM) in Ca<sup>2+</sup>-free buffer followed by replenishment of 2 mM external Ca<sup>2+</sup>. Dashed rectangle indicates SOCE.

<https://doi.org/10.1371/journal.pone.0183114.g005>

should be attributed to metabotropic G protein-coupled P2Y receptors, rather than ionotropic P2X channels [20]. Among P2Y subtypes expressed in BV-2 microglia (P2Y<sub>2, 6, 12, 13, 14</sub>; Fig 4H and 4I), UTP could activate P2Y<sub>2</sub> receptors, UDP activated P2Y<sub>6</sub> and UDP-glucose targeted for P2Y<sub>14</sub> [21, 22]. In view of the negative effects for these three nucleotides in ICWs (Fig 4B to 4D), P2Y<sub>2,6,14</sub> could be excluded from the candidate receptors mediating ICWs. On the other hand, the predominantly expressed P2Y<sub>12/13</sub> receptors, could be activated by both ATP and ADP [21, 22]. Our data showed that desensitizing by ATP/ADP and application of MRS2395/MRS2211 could all eliminate ICWs. Therefore, it determined the pivotal roles of P2Y<sub>12/13</sub> receptors in ICW communication between BV-2 cells. In addition, although ATP cannot activate P2Y<sub>12/13</sub> receptors directly [32, 33], membrane-localized ecto-NTPase usually catalyzes hydrolysis of ATP and generates ADP that predominantly activates P2Y<sub>12/13</sub> receptors [32, 34–36]. Thus, inhibition of ecto-NTPase with ARL 67156 suppressed the ICW propagation in BV-2 microglia (S3 Fig). We summarized an ATP/ADP-P2Y<sub>12/13</sub>R-PLC-IP<sub>3</sub>-Ca<sup>2+</sup> signaling pathway for mechanical stimulation-induced ICWs by a diagram (Fig 6).

This mechanism we proposed was differ from previous studies, such as P2Y<sub>1,2</sub> receptors mediated ICWs in rat astrocytes [37], P2Y<sub>11</sub> receptors contributed to ICWs in rat cardiac myofibroblasts [38] and N-methyl-D-aspartic acid (NMDA) receptor was involved in zebrafish microglial ICWs [15]. Importantly, in addition to participate in ICWs, extracellular nucleotides were associated with a wide array of physiological effects of microglia through activation of specific P2 receptors [39]. For instance, P2X<sub>7</sub> receptors are relevant to membrane pore

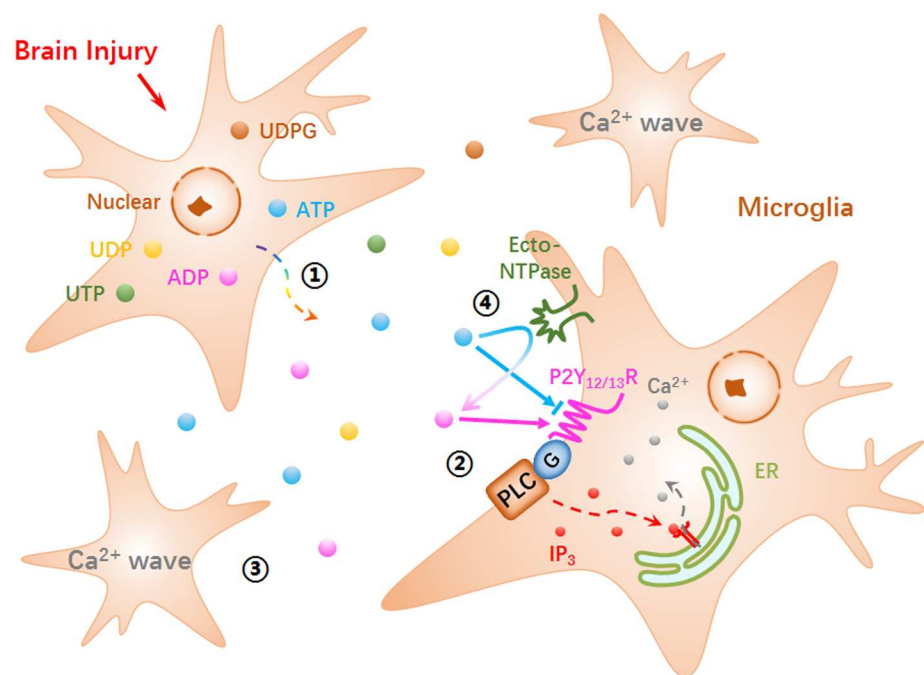


**Fig 6. Mechanism underlying mechanical stimulation-elicited ICWs among BV-2 microglia.** ① A range of nucleotides, including ATP, ADP and UDP etc., are released into extracellular space in response to mechanical stimulus. ② P2Y<sub>12/13</sub> receptors localized on the membrane of neighboring cells can sense ATP/ADP released from the stimulated cell, then activate PLC/IP<sub>3</sub>/Ca<sup>2+</sup> signaling. ③ Upon sensing and responding to released ATP/ADP, Ca<sup>2+</sup> mobilization sequentially occur in neighboring cells, thus perform as intercellular calcium waves. ④ ATP cannot activate P2Y<sub>12/13</sub> receptors directly. Ecto-NTPase located on the plasma membrane could catalyze hydrolysis of ATP and generates ADP that predominantly activates P2Y<sub>12/13</sub> receptors.

<https://doi.org/10.1371/journal.pone.0183114.g006>

formation, microvesicle shedding and cell apoptosis [40, 41]. P2X<sub>4</sub> as well as P2Y<sub>12</sub> receptors mediated microglial chemotaxis toward injured sites [42–44], and P2Y<sub>6</sub> receptor was critical player in promoting microglial phagocytosis resulted from Ca<sup>2+</sup> mobilization [34].

Metabolic G protein-coupled P2Y receptors are divided into two classes: G<sub>q</sub> protein-coupled receptors, mainly P2Y<sub>1-11</sub> receptors, and G<sub>i</sub>-coupled P2Y<sub>12-14</sub> receptors. Activation of G<sub>q</sub>-protein could stimulate phospholipase C β (PLCβ), then cleave PIP<sub>2</sub> into two types of second messengers IP<sub>3</sub> and DAG, and triggered Ca<sup>2+</sup> mobilization [45]. In contrast, activation of G<sub>i</sub>-coupled P2Y<sub>12/13</sub> receptors inhibited the adenylate cyclase (AC)/cAMP-dependent pathway [44]. Meanwhile, G<sub>i</sub>-coupled P2Y<sub>12/13</sub> receptors resulted in activation of the phosphatidylinositol 3'-kinase (PI3K) pathway, which was known to be a crucial enzyme in the regulation of chemotaxis [46]. Nevertheless, some studies reported that activation of P2Y<sub>12/13</sub> receptor could also mediate PLC/IP<sub>3</sub>/Ca<sup>2+</sup> pathway [47, 48]. Our study indicated the correlation between PLC/IP<sub>3</sub>/Ca<sup>2+</sup> signaling and P2Y<sub>12/13</sub> receptors, which were consistent with de Simone's [48] and Zeng's work [49].

Subsequently, we estimated the concentrations of paracrine ATP and ADP sensed by BV-2 microglia during the ICW. The traditional method detecting concentration of ATP was luciferin-luciferase assay. However, this method was mostly used for the measurements of the overall level of ATP concentration and not applicable to ADP. In this work, we found that mechanical stimulation-evoked ICWs was due to calcium release rather than SOCE (Fig 5A). Therefore, we observed whether the [Ca<sup>2+</sup>]<sub>c</sub> pattern in response to exogenous ATP and ADP at different concentration were in agreement with mechanical stimulation-induced ICW. Data showed that different concentration of nucleotides could induce different patterns of Ca<sup>2+</sup> transient, which was similar to that of Visentin's work [50]. Only application of 0.3 μM ATP or ADP exhibited a similar characteristic behavior to that of mechanical stimulation-evoked ICWs (Fig 5C and 5E), indicating that the concentration of ATP and ADP sensed by purinergic receptors of BV-2 microglia was about 0.3 μM. These findings might be significant in the field of drug analysis and development and could provide the basis for pharmacological experiments.

One of the main limitation on this study was the application of BV-2 microglia. Although BV-2 has been known as an immortalized mouse microglial cell line that exhibits the morphological and functional characteristics of primary microglia [19, 51], there is no denying that it cannot fully represent the real physiological features of primary microglia *in situ* or *in vivo* [52]. Therefore, we plan to study and understand the procedure of primary microglia isolation. Much work will be performed on primary microglia that makes our research more interesting and significant.

In summary, our study demonstrated that ATP and ADP were predominant signal transmitters in mechanical stimulation-induced ICWs through P2Y<sub>12/13</sub> receptors activation in BV-2 microglia. The concentration of ATP/ADP sensed by BV-2 microglia was about 0.3 μM. Our research may bring new insights in the mechanism of cell-to-cell communication of microglia to investigation of its immune defense in the CNS.

## Supporting information

**S1 Movie. Intercellular calcium wave triggered by mechanical stimulus in BV-2 microglia.**  
(AVI)

**S1 Fig. BV-2 microglia maintain or lose plasma membrane integrity after different mechanical stimulations.**  
(DOCX)

**S2 Fig. Desensitization of purinoceptors by application of ATP and ADP.**  
(DOCX)

**S3 Fig. Ectonucleotidase inhibitor ARL 67156 significantly blocks the ICW propagations in BV-2 microglia.**  
(DOCX)

**S1 Table. Primers used to detect P2Y receptor genes in BV-2 microglia in RT-PCR.**  
(DOCX)

## Acknowledgments

This work was supported by the National Natural Science Foundation of China (No. 11574165), Program for Changjiang Scholars and Innovative Research Team in University (No. IRT\_13R29), the 111 Project (No. B07013).

## Author Contributions

**Conceptualization:** Fulin Xing.

**Data curation:** Pengchong Jiang, Fulin Xing, Bu Guo, Jianyu Yang, Zheming Li.

**Formal analysis:** Pengchong Jiang, Fulin Xing, Bu Guo, Jianyu Yang, Zheming Li, Wei Wei.

**Funding acquisition:** Xinzheng Zhang, Leiting Pan, Jingjun Xu.

**Investigation:** Pengchong Jiang, Fulin Xing, Leiting Pan.

**Methodology:** Pengchong Jiang.

**Project administration:** Fen Hu, Leiting Pan.

**Resources:** Imshik Lee, Xinzheng Zhang, Leiting Pan, Jingjun Xu.

**Supervision:** Leiting Pan, Jingjun Xu.

**Validation:** Pengchong Jiang, Fulin Xing.

**Visualization:** Pengchong Jiang, Fulin Xing, Bu Guo.

**Writing – original draft:** Pengchong Jiang, Fen Hu.

**Writing – review & editing:** Leiting Pan.

## References

1. Ferrari D, McNamee EN, Idzko M, Gambari R, Eltzschig HK. Purinergic signaling during immune cell trafficking. *Trends Immunol.* 2016; 37(6):399–411. <https://doi.org/10.1016/j.it.2016.04.004> PMID: 27142306
2. Cekic C, Linden J. Purinergic regulation of the immune system. *Nat Rev Immunol.* 2016; 16(3):177–192. <https://doi.org/10.1038/nri.2016.4> PMID: 26922909
3. Chen Y, Corriden R, Inoue Y, Yip L, Hashiguchi N, Zinkernagel A, et al. ATP release guides neutrophil chemotaxis via P2Y<sub>2</sub> and A<sub>3</sub> receptors. *Science.* 2006; 314(5806):1792–1795. <https://doi.org/10.1126/science.1132559> PMID: 17170310
4. Elliott MR, Cheleni FB, Tramont PC, Lazarowski ER, Kadl A, Walk SF, et al. Nucleotides released by apoptotic cells act as a find-me signal to promote phagocytic clearance. *Nature.* 2009; 461(7261):282–286. <https://doi.org/10.1038/nature08296> PMID: 19741708
5. Burnstock G. An introduction to the roles of purinergic signalling in neurodegeneration, neuroprotection and neuroregeneration. *Neuropharmacology.* 2016; 104:4–17. <https://doi.org/10.1016/j.neuropharm.2015.05.031> PMID: 26056033



6. Neher JJ, Neniskyte U, Hornik T, Brown GC. Inhibition of UDP/P2Y<sub>6</sub> purinergic signaling prevents phagocytosis of viable neurons by activated microglia *in vitro* and *in vivo*. *Glia*. 2014; 62(9):1463–1475. <https://doi.org/10.1002/glia.22693> PMID: 24838858
7. Hechler B, Gachet C. Purinergic receptors in thrombosis and inflammation. *Arterioscler Thromb Vasc Biol*. 2015; 35(11):2307–2315. <https://doi.org/10.1161/ATVBAHA.115.303395> PMID: 26359511
8. Li W, Tong HI, Gorantla S, Poluektova LY, Gendelman HE, Lu Y. Neuropharmacologic approaches to restore the brain's microenvironment. *J Neuroimmune Pharmacol*. 2016; 11(3):484–494. <https://doi.org/10.1007/s11481-016-9686-5> PMID: 27352074
9. Eichhoff G, Brawek B, Garaschuk O. Microglial calcium signal acts as a rapid sensor of single neuron damage *in vivo*. *Biochim Biophys Acta*. 2011; 1813(5):1014–1024. <https://doi.org/10.1016/j.bbamcr.2010.10.018> PMID: 21056596
10. Davalos D, Grutzendler J, Yang G, Kim JV, Zuo Y, Jung S, et al. ATP mediates rapid microglial response to local brain injury *in vivo*. *Nat Neurosci*. 2005; 8(6):752–758. <https://doi.org/10.1038/nn1472> PMID: 15895084
11. Samuels SE, Lipitz JB, Dahl G, Muller KJ. Neuroglial ATP release through innexin channels controls microglial cell movement to a nerve injury. *J Gen Physiol*. 2010; 136(4):425–442. <https://doi.org/10.1085/jgp.201010476> PMID: 20876360
12. Wu X, Pan L, Liu Y, Jiang P, Lee I, Drevensek-Olenik I, et al. Cell-cell communication induces random spikes of spontaneous calcium oscillations in multi-BV-2 microglial cells. *Biochem Biophys Res Commun*. 2013; 431(4):664–669. <https://doi.org/10.1016/j.bbrc.2013.01.064> PMID: 23357419
13. Pires M, Raischel F, Vaz SH, Cruz-Silva A, Sebastião AM, Lind PG. Modeling the functional network of primary intercellular Ca<sup>2+</sup> wave propagation in astrocytes and its application to study drug effects. *J Theor Biol*. 2014; 356:201–212. <https://doi.org/10.1016/j.jtbi.2014.04.024> PMID: 24813072
14. Zeng Y, Lv XH, Zeng SQ, Tian SL, Li M, Shi J. Sustained depolarization-induced propagation of [Ca<sup>2+</sup>]<sub>i</sub> oscillations in cultured DRG neurons: the involvement of extracellular ATP and P2Y receptor activation. *Brain Res*. 2008; 1239:12–23. <https://doi.org/10.1016/j.brainres.2008.08.085> PMID: 18804455
15. Sieger D, Moritz C, Ziegenhals T, Prykhodzhiy S, Peri F. Long-range Ca<sup>2+</sup> waves transmit brain-damage signals to microglia. *Dev Cell*. 2012; 22(6):1138–1148. <https://doi.org/10.1016/j.devcel.2012.04.012> PMID: 22632801
16. Cotrina ML, Lin JH, López-García JC, Naus CC, Nedergaard M. ATP-mediated glia signaling. *J Neurosci*. 2000; 20(8):2835–2844. PMID: 10751435
17. Schipke CG, Boucsein C, Ohlemeyer C, Kirchhoff F, Kettenmann H. Astrocyte Ca<sup>2+</sup> waves trigger responses in microglial cells in brain slices. *FASEB J*. 2002; 16(2):255–257. <https://doi.org/10.1096/fj.01-0514fje> PMID: 11772946
18. Verderio C, Matteoli M. ATP mediates calcium signaling between astrocytes and microglial cells: modulation by IFN-γ. *J Immunol*. 2001; 166(10):6383–6391. PMID: 11342663
19. Gordon R, Singh N, Lawana V, Ghosh A, Harischandra DS, Jin H, et al. Protein kinase Cδ upregulation in microglia drives neuroinflammatory responses and dopaminergic neurodegeneration in experimental models of Parkinson's disease. *Neurobiol Dis*. 2016; 93:96–114. <https://doi.org/10.1016/j.nbd.2016.04.008> PMID: 27151770
20. James G, Butt AM. P2Y and P2X purinoceptor mediated Ca<sup>2+</sup> signalling in glial cell pathology in the central nervous system. *Eur J Pharmacol*. 2002; 447(2–3):247–260. PMID: 12151016
21. von Kügelgen I. Pharmacological profiles of cloned mammalian P2Y-receptor subtypes. *Pharmacol Ther*. 2006; 110(3):415–432. <https://doi.org/10.1016/j.pharmthera.2005.08.014> PMID: 16257449
22. Jacobson KA, Ivanov AA, de Castro S, Harden TK, Ko H. Development of selective agonists and antagonists of P2Y receptors. *Purinergic Signal*. 2009; 5(1):75–89. <https://doi.org/10.1007/s11302-008-9106-2> PMID: 18600475
23. Weissman TA, Riquelme PA, Ivic L, Flint AC, Kriegstein AR. Calcium waves propagate through radial glial cells and modulate proliferation in the developing neocortex. *Neuron*. 2004; 43(5):647–661. <https://doi.org/10.1016/j.neuron.2004.08.015> PMID: 15339647
24. Khakh BS, Burnstock G. The double life of ATP. *Sci Am*. 2009; 301(6):84–90. PMID: 20058644
25. Fredholm B, Verkhratsky A. Purines—80 years and very much alive. *Acta Physiol (Oxf)*. 2010; 199(2):91–92. <https://doi.org/10.1111/j.1748-1716.2010.02113.x> PMID: 20534039
26. Lohman AW, Billaud M, Isakson BE. Mechanisms of ATP release and signalling in the blood vessel wall. *Cardiovasc Res*. 2012; 95(3):269–280. <https://doi.org/10.1093/cvr/cvs187> PMID: 22678409
27. Lazarowski ER. Vesicular and conductive mechanisms of nucleotide release. *Purinergic Signal*. 2012; 8(3):359–373. <https://doi.org/10.1007/s11302-012-9304-9> PMID: 22528679

28. Lazarowski ER, Sesma JI, Seminario-Vidal L, Kreda SM. Molecular mechanisms of purine and pyrimidine nucleotide release. *Adv Pharmacol.* 2011; 61:221–261. <https://doi.org/10.1016/B978-0-12-385526-8.00008-4> PMID: 21586361
29. Piazza V, Ciubotaru CD, Gale JE, Mammano F. Purinergic signalling and intercellular Ca<sup>2+</sup> wave propagation in the organ of Corti. *Cell Calcium.* 2007; 41(1):77–86. <https://doi.org/10.1016/j.ceca.2006.05.005> PMID: 16828497
30. Hausmann R, Kless A, Schmalzing G. Key sites for P2X receptor function and multimerization: overview of mutagenesis studies on a structural basis. *Curr Med Chem.* 2015; 22(7):799–818. <https://doi.org/10.2174/0929867322666141128163215> PMID: 25439586
31. Ma L, Pei G. Beta-arrestin signaling and regulation of transcription. *J Cell Sci.* 2007; 120(Pt 2):213–218. <https://doi.org/10.1242/jcs.03338> PMID: 17215450
32. Kauffenstein G, Hechler B, Cazenave JP, Gachet C. Adenine triphosphate nucleotides are antagonists at the P2Y receptor. *J Thromb Haemost.* 2004; 2(11):1980–1988. <https://doi.org/10.1111/j.1538-7836.2004.00926.x> PMID: 15550030
33. Raboisson P, Baurand A, Cazenave JP, Gachet C, Schultz D, Spiess B. A general approach toward the synthesis of C-nucleoside pyrazolo [1,5-a]-1,3,5-triazines and their 3',5'-bisphosphate C-nucleotide analogues as the first reported in vivo stable P2Y<sub>1</sub>-receptor antagonists. *J Org Chem.* 2002; 67(23):8063–8071. PMID: 12423133
34. Hechler B, Vigne P, Léon C, Breittmayer JP, Gachet C, Frelin C. ATP derivatives are antagonists of the P2Y<sub>1</sub> receptor: similarities to the platelet ADP receptor. *Mol Pharmacol.* 1998; 53(4):727–733. PMID: 9547364
35. Léon C, Hechler B, Vial C, Leray C, Cazenave JP, Gachet C. The P2Y<sub>1</sub> receptor is an ADP receptor antagonized by ATP and expressed in platelets and megakaryoblastic cells. *FEBS Lett.* 1997; 403(4):26–30. PMID: 9038354
36. Light AR, Wu Y, Hughen RW, Guthrie PB. Purinergic receptors activating rapid intracellular Ca increases in microglia. *Neuron Glia Biol.* 2006; 2(2):125–138. <https://doi.org/10.1017/S1740925X05000323> PMID: 16652167
37. Rodrigues RJ, Tomé AR, Cunha RA. ATP as a multi-target danger signal in the brain. *Front Neurosci.* 2015; 9:148. <https://doi.org/10.3389/fnins.2015.00148> PMID: 25972780
38. Certal M, Vinhas A, Pinheiro AR, Ferreirinha F, Barros-Barbosa AR, Silva I, et al. Calcium signaling and the novel anti-proliferative effect of the UTP-sensitive P2Y<sub>11</sub> receptor in rat cardiac myofibroblasts. *Cell Calcium.* 2015; 58(5):518–533. <https://doi.org/10.1016/j.ceca.2015.08.004> PMID: 26324417
39. Cavaliere F, Donno C, D'Ambrosi N. Purinergic signaling: a common pathway for neural and mesenchymal stem cell maintenance and differentiation. *Front Cell Neurosci.* 2015; 9:211. <https://doi.org/10.3389/fncel.2015.00211> PMID: 26082684
40. Monif M, Reid CA, Powell KL, Smart ML, Williams DA. The P2X<sub>7</sub> receptor drives microglial activation and proliferation: a trophic role for P2X<sub>7</sub>R pore. *J Neurosci.* 2009; 29(12):3781–3791. <https://doi.org/10.1523/JNEUROSCI.5512-08.2009> PMID: 19321774
41. Wilson HL, Francis SE, Dower SK, Crossman DC. Secretion of intracellular IL-1 receptor antagonist (type 1) is dependent on P2X<sub>7</sub> receptor activation. *J Immunol.* 2004; 173(2):1202–1208. PMID: 15240711
42. Haynes SE, Hollopeter G, Yang G, Kurpius D, Dailey ME, Gan WB, et al. The P2Y<sub>12</sub> receptor regulates microglial activation by extracellular nucleotides. *Nat Neurosci.* 2006; 9(12):1512–1519. <https://doi.org/10.1038/nn1805> PMID: 17115040
43. Ohsawa K, Irino Y, Nakamura Y, Akazawa C, Inoue K, Kohsaka S. Involvement of P2X<sub>4</sub> and P2Y<sub>12</sub> receptors in ATP-induced microglial chemotaxis. *Glia.* 2007; 55(6):604–616. <https://doi.org/10.1002/glia.20489> PMID: 17299767
44. Irino Y, Nakamura Y, Inoue K, Kohsaka S, Ohsawa K. Akt activation is involved in P2Y<sub>12</sub> receptor-mediated chemotaxis of microglia. *J Neurosci Res.* 2008; 86(7):1511–1519. <https://doi.org/10.1002/jnr.21610> PMID: 18183622
45. Sandal M, Paltrinieri D, Carloni P, Musiani F, Giorgetti A. Structure/function relationships of phospholipases C Beta. *Curr Protein Pept Sci.* 2013; 14(8):650–657 PMID: 24384033
46. Honda S, Sasaki Y, Ohsawa K, Imai Y, Nakamura Y, Inoue K, et al. Extracellular ATP or ADP induce chemotaxis of cultured microglia through Gi/o-coupled P2Y receptors. *J Neurosci.* 2001; 21(6):1975–1982. PMID: 11245682
47. Obál FJ, Krueger JM. The somatotrophic axis and sleep. *Rev Neurol.* 2001; 157:S12–15. PMID: 11924022

48. De Simone R, Niturad CE, De Nuccio C, Ajmone-Cat MA, Visentin S, Minghetti L. TGF- $\beta$  and LPS modulate ADP-induced migration of microglial cells through P2Y1 and P2Y12 receptor expression. *J Neurochem*. 2010; 115(2):450–459. <https://doi.org/10.1111/j.1471-4159.2010.06937.x> PMID: 20681951
49. Zeng J, Wang G, Liu X, Wang C, Tian H, Liu A, et al. P2Y13 receptor-mediated rapid increase in intracellular calcium induced by ADP in cultured dorsal spinal cord microglia. *Neurochem Res*. 2014; 39(11):2240–2250. <https://doi.org/10.1007/s11064-014-1426-8> PMID: 25186167
50. Visentin S, Nuccio CD, Belenchi GC. Different patterns of Ca<sup>2+</sup> signals are induced by low compared to high concentrations of P2Y agonists in microglia. *Purinergic Signal*. 2006; 2(4):605–617. <https://doi.org/10.1007/s11302-006-9023-1> PMID: 18404463
51. Cao Q, Lu J, Kaur C, Sivakumar V, Li F, Cheah PS, et al. Expression of Notch-1 receptor and its ligands Jagged-1 and Delta-1 in amoeboid microglia in postnatal rat brain and murine BV-2 cells. *Glia*. 2008; 56(11):1224–1237. <https://doi.org/10.1002/glia.20692> PMID: 18449946
52. Horvath RJ, Nutile-McMenemy N, Alkaitis MS, Deleo JA. Differential migration, LPS-induced cytokine, chemokine, and NO expression in immortalized BV-2 and HAPI cell lines and primary microglial cultures. *J Neurochem*. 2008; 107(2):557–569. <https://doi.org/10.1111/j.1471-4159.2008.05633.x> PMID: 18717813